Colorimetric Chiral Recognition of Enantiomers Using the Nucleotide-Capped Silver Nanoparticles

ARTICLE *in* ANALYTICAL CHEMISTRY · FEBRUARY 2011

Impact Factor: 5.64 · DOI: 10.1021/ac102922f · Source: PubMed

2 AUTHORS:

Min Zhang
East China Normal University
36 PUBLICATIONS **920** CITATIONS
SEE PROFILE

Bang-Ce Ye
East China University of Science and Techno…
134 PUBLICATIONS **2,344** CITATIONS
SEE PROFILE

analytical chemistry

LETTER

pubs.acs.org/ac

Colorimetric Chiral Recognition of Enantiomers Using the Nucleotide-Capped Silver Nanoparticles

Min Zhang and Bang-Ce Ye*

Lab of Biosystems and Microanalysis, State Key Laboratory of Bioreactor Engineering, East China University of Science and Technology, Meilong Road 130, Shanghai, 200237, China

Supporting Information

ABSTRACT: Chiral recognition is among the important and special modes of molecular recognition. It is highly desirable to develop a simple, rapid, sensitive, and high-throughput routine assay for chiral recognition. In this study, we demonstrate that nucleotide-capped Ag nanoparticles (AgNPs) can be used as an ultrahigh efficiency enantioseparation and detection platform for D- and L-cysteine. The aggregation of AgNPs is selectively induced by an enantiomer of cysteine, which allowed the rapid colorimetric enantiodiscrimination of cysteine without any prior derivatization and specific instruments and left an excess of the other enantiomer in the solution, thus resulting in enantioseparation. This is the first application of a nucleotide-capped AgNP-based biosensing platform for chiral recognition and opens new opportunities for design of more novel enantiosensing strategies and enantiospecific adsorbents and expansion of its application in different fields.

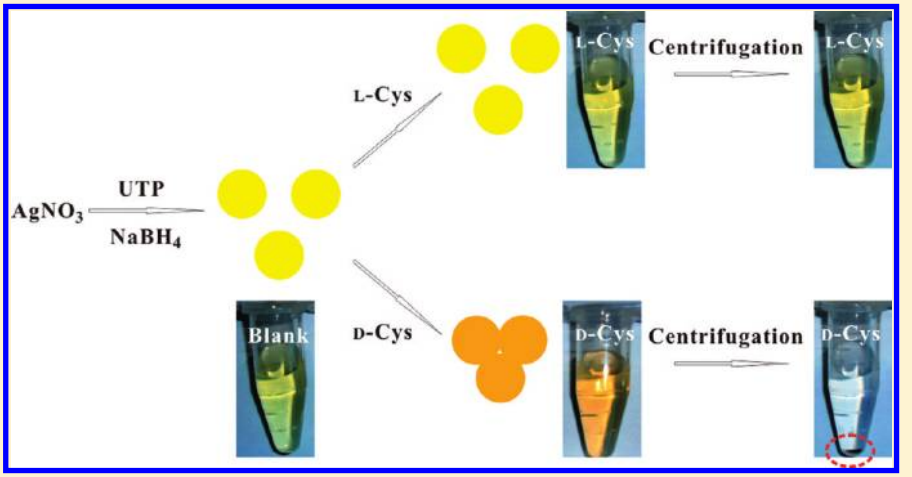

Chiral recognition is among the important and special modes of molecular recognition, which draws extensive attention in the field of biochemistry, pharmaceutics, and drug development. Chirality is the basic characteristics of life processes, and majorities of organic molecules, the element of living things, are chiral molecules. Most of the drugs also have chirality. The performance of the enantiomers of a chiral molecule may exhibit remarkable discrepancy in terms of biochemical activity, potency, toxicity, transport mechanism, and pathways of metabolism. The development of a means of discriminating between enantiomers of a chiral molecule is of critical importance in many fields of analytical chemistry and biotechnology, especially in pharmaceutical science and technology. Over the past decades, many methods for distinguishing chiral molecules have been reported, such as chiral HPLC (high-performance liquid chromatography), GC (gas chromatography), CE (capillary electrophoresis), etc.,[1] but most of them are time-consuming and impractical for a real-time, multiplex, or high-throughput format. Therefore, it is still highly desirable to develop a simple, rapid, sensitive, and high-throughput routine assay for chiral recognition, in particular, solution-based sensor systems capable of chiral recognition will be of tremendous pharmaceutical value.[2] One of the most pressing challenges in the design of solution-based sensor systems is to achieve visual discrimination of enantiomers. An ideal sensor that achieves this would have to translate an enantioselective molecular recognition event into an appreciable color change.[3] Recent years have witnessed the development of a colorimetric assay utilizing metal nanoparticles (NPs) as a sensing element based on its unique surface plasmon resonance properties. The metal NP-based colorimetric sensors, due to simplicity, high sensitivity, and lower cost, have been widely developed for detecting various analytes including oligonucleotides,[4] small molecules,[5] proteins,[6] carbohydrates,[7] and metal ions[8] in homogeneous solutions, which depend on the targeted analyte-induced reversible color switch between dispersion−aggregation states of NPs. Without the need of advanced instruments, yet just easily monitored by the naked eye, this colorimetric assay is increasingly becoming a routine bioassay that could provide comparable or even higher sensitivity and better selectivity than conventional molecular fluorescent ones. It is known that metal nanoparticle surfaces can exhibit intrinsically chiral structure.

Received: November 7, 2010
Accepted: January 30, 2011
Published: February 08, 2011

Furthermore, chirality can be bestowed onto achiral metal surfaces by adsorption of chiral molecules.[9] Recently, the chirality of these metal nanoparticles has attracted attention, and application to chiral technologies is an interesting perspective. The considerable effort has been devoted to the synthesis and characterization of chiral, optically active ligand-capped metal nanoparticles.[10] However, the field of enantioselective recognition using metal nanoparticles still remains unexplored.

Herein, we presented, for the first time, a simple and reliable colorimetric method for the separation and quantitative determination of enantiomers in aqueous solution using uridine 5′-triphosphate (UTP)-capped silver nanoparticles (AgNPs) without any prior derivatization and sample preparation. AgNPs reveal a distance-relevant color and higher extinction coefficient than that of AuNPs in the same size,[11] which entitles them to be acted as ideal color reporting elements for colorimetric sensor design. In the previous literature, AgNPs are usually prepared by reducing $AgNO_3$ with citrate sodium by sodium borohydride, and the resulting nanoparticles are capped with the citrate group. Moreover, some capping agents were utilized to stabilize AgNPs.[12] Nucleotides are reported to be capable of interacting with metal ions via nucleobases and a phosphodiester backbone,[13] and the different nucleotides have diverse affinities to metal nanoparticles.[14] UTP consists of uridine and three phosphate groups, which suggests that it can serve as an effective capping ligand during the nanoparticles growth process: uridine can bind to nanoparticle surfaces due to the interaction between functional groups (amines, carbonyls) of the nucleobases and the metal surface, and the negatively charged phosphate group can stabilize the nanoparticles against aggregation in the phase of its growth through electrostatic repulsion. In this study, as a model system, L- and D-cysteine (Cys) were used to evaluate the UTP-capped AgNPs on the colorimetric discrimination of chiral enantiomers because of their biological importance and their inherent chiral structure.[15]

EXPERIMENTAL SECTION

Reagents and Materials. Adenosine 5′-triphosphate (ATP), guanosine 5′-triphosphate (GTP), cytidine 5′-triphosphate (CTP), uridine 5′-triphosphate (UTP), L-cysteine, and D-cysteine were purchased from Sigma-Aldrich (St. Louis, MO). Sodium borohydride ($NaBH_4$) was obtained from Tianlian Fine Chemical Co., Ltd. (Shanghai, China). Silver nitrate ($AgNO_3$) was obtained from Sinopharm Chemical Reagent Co. Ltd. (Shanghai, China). All chemicals used in this work were of analytical reagent, obtained from commercial sources, and directly used without additional purification. $NaNO_3$−MOPS buffer (10×, 500 mM $NaNO_3$, 200 mM 3-morpholinopropane-1-sulfonic acid, pH 7.0) was prepared using metal-free reagents in distilled water purified by a Milli-Q water purification system (Millipore Corp., Bedford, MA) with an electrical resistance of 18.2 MΩ. All glassware was thoroughly cleaned overnight with freshly prepared 3:1 HCl/HNO_3 (aqua regia) and rinsed thoroughly with Mill-Q water prior to use. All buffer solutions and ultrapure water were sterilized and used throughout the experiments.

Instrumentation. The ultraviolet visible (UV−vis) absorption spectrum was recorded with a microplate reader (BioTek Instruments, Winooski, VT, USA) with wavelength ranging from 300 to 700 nm using a transparent 384-well microplate (Greiner, Germany). Photographs were taken with a SONY DSC-W300 digital camera (Tokyo, Japan).

Typical Synthesis of Nucleotide-Capped AgNPs. $AgNO_3$ (62.5 μL of 0.1 M) and 62.5 μL of 0.1 M UTP (or ATP, GTP, or CTP) were mixed. The mixture was incubated for 30 min at room temperature and then was added into 25 mL of ddH_2O under stirring in a 50 mL glass vial. Freshly prepared $NaBH_4$ (5 mM, 1.5 mL) was then quickly added into the above aqueous solution under vigorous stirring. The resulting colloidal silver solution was stirring for 30 min and then was stored at 4 °C overnight to ensure the completion of AgNP growth before further use.

Colorimetric Chiral Recognition. An aliquot of 90 μL UTP-capped AgNPs in aqueous $NaNO_3$ (50 mM) and 3-(4-morpholinyl)-1-propanesulfonic acid (MOPS) buffer (20 mM, pH 7.0) was placed in the wells of a transparent 384-well microtiter plate. Then, 10 μL of L-Cys, D-Cys, or ddH_2O was added to the corresponding wells. Subsequently, the absorption reading was begun immediately following a 60 min period and a 3 min interval at RT. The experiments of optimization of sensing conditions were carried out under identical conditions. All experiments were repeated two times.

RESULTS AND DISCUSSION

Scheme 1 presents the homogeneous enantioselective strategy of the use of UTP-capped AgNPs for the colorimetric discrimination of chiral enantiomers on the basis of absorption chemistry. In the presence of D-Cys, an appreciable yellow-to-red color shift of UTP-capped AgNPs can be observed. However, no color changes were found in the presence of L-Cys. More importantly, UTP-capped AgNPs selectively interacted with one enantiomer of cysteine from a solution of racemic cysteine, leaving an excess of the other enantiomer in the solution after centrifugation treatment, thus resulting in enantioselective separation.

The enantioselective interaction of chiral cysteine with UTP-capped AgNPs can also be probed using UV−vis absorbance spectroscopy. As a proof-of-principle experiment, an aliquot of UTP-capped AgNPs in aqueous $NaNO_3$ (50 mM) and 3-(4-morpholinyl)-1-propanesulfonic acid (MOPS) buffer (20 mM, pH 7.0) was placed in the wells of a transparent 384-well microtiter plate. An aqueous solution of L- or D-Cys (100 μM) was added to each well, and then, the absorption properties were kinetically monitored. As shown in Figure 1, time-course absorption behavior of UTP-capped AgNPs toward D-Cys is strikingly different from that of L-Cys. An absorption peak was observed at 400 nm that originates from the surface plasmon absorption of AgNPs; upon the addition of D-cysteine, the absorption peak red-shifted to 520 nm, and the color of the solution was changed from yellow to red (Figure 1C). D-Cys-induced aggregation of UTP-capped AgNPs resulted in a decrease in the plasmon absorption at 400 nm and the formation of a broadened surface plasmon band around 450−600 nm. No L-Cys-induced aggregation was found, as evidenced by the fact that there is no color change and significant UV−vis spectral shift (Figure 1B). Considering the ratios of the absorbance at 520 and 400 nm (A_{520}/A_{400}) are related to the quantities of dispersed and aggregated AgNPs, we chose A_{520}/A_{400} as the indicator of the performance of AgNPs. Figure 1D illustrates the significant difference in the absorbance ratio A_{520}/A_{400} of UTP-capped AgNPs responding to L- and D-cysteine over periods of 60 min.

The UTP-capped AgNP-based colorimetric assay is sensitive to D-Cys. Calibration of the absorbance ratio (A_{520}/A_{400}) using enantiomerically pure L- or D-Cys in aqueous solution at

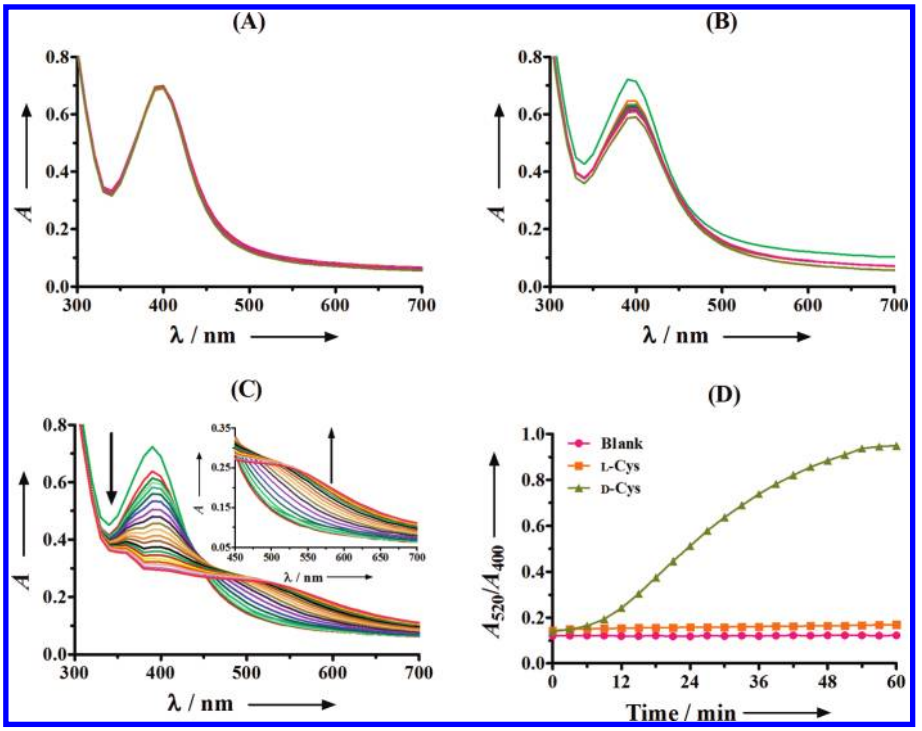

Figure 1. Time-course study on UV−vis absorbance of UTP-capped AgNPs in solution upon addition of (A) H_2O as a blank, (B) 100 μM L-Cys, and (C) 100 μM D-Cys; (D) plots of absorption ratios (A_{520}/A_{400}) corresponding to H_2O, 100 μM L-Cys, and 100 μM D-Cys.

Scheme 1. Colorimetric Discrimination of L- and D-Cys Using UTP-Capped AgNPs

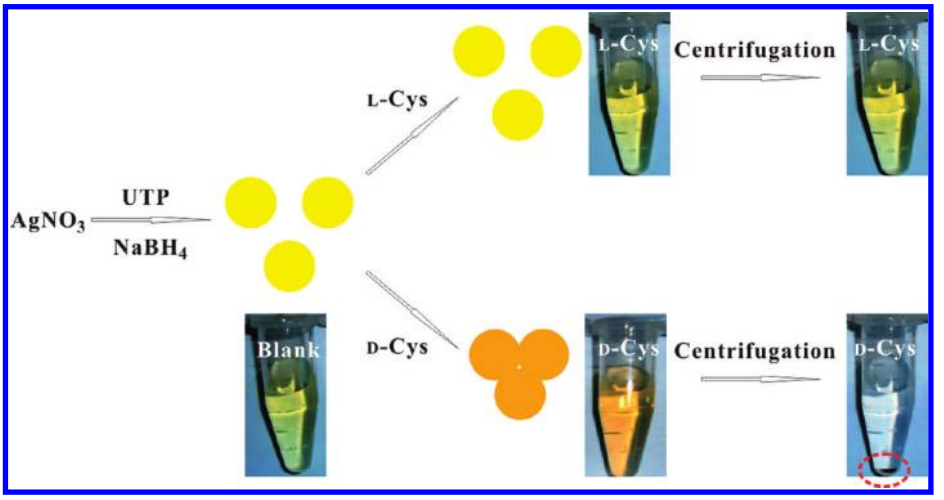

concentrations up to 10 mM is shown in Figure 2. A dramatic increase in the A_{520}/A_{400} ratio of UTP-capped AgNPs was observed in the presence of D-Cys concentration increasing from 0.1 to 100 μM; however, in the same condition, the A_{520}/A_{400} ratio of UTP-capped AgNPs toward L-Cys almost kept a lower unchanged value. The spectral change was not detectable in 60 min at a concentration of 100 μM for L-Cys (Figure 1B). However, when the concentration of L-Cys exceeds 100 μM, the resulting A_{520}/A_{400} ratio also increases; especially, around 1000 μM, the resulting A_{520}/A_{400} ratio is equal to that of D-Cys, which is probably due to the fact that the high concentration of Cys makes the UTP-capped AgNPs unstable and then aggregate. The data indicated that the aggregation induced by D-Cys is much more sensitive than by L-Cys by at least 2 orders of magnitude. The limit of discrimination concentration between L- and D-Cys is approximately 100 nM. It is reasonable to believe that the UTP-capped AgNP-based colorimetric assay is capable of discriminating trace chiral enantiomers.

The solutions of UTP-capped AgNPs mixed with L- or D-Cys (100 μM, 60 min) were centrifuged at 12 000 rpm for 5 min. A lot of precipitate can be collected in the bottom of tube which contains UTP-capped AgNPs and D-Cys; however, no obvious changes occurred in the L-Cys tube under the same condition (Figure 3A,B). To test the feasibility of the UTP-capped AgNPs as enantiospecific adsorbents, the resultant supernatant in D-Cys tube was again interacted with UTP-capped AgNPs. In this case,

dx.doi.org/10.1021/ac102922f |*Anal. Chem.* 2011, 83, 1504–1509

no colorimetric change was observed, and the significant UV−vis spectral shift (A_{520}/A_{400}) was also not detectable (Figure 3C). The results in Figure 3 suggest that D-cysteine can selectively induce the aggregation of UTP-capped AgNPs and can be precipitated with AgNPs via the interfacial encapsulation and cross-linking reaction. The work reveals the potential of UTP-capped AgNPs to serve as enantiospecific adsorbents of chiral species. To further confirm an enantioselective separation and enantiomeric purification of the cysteine utilizing AgNPs, we applied UTP-capped AgNPs to the racemic cysteine solution.

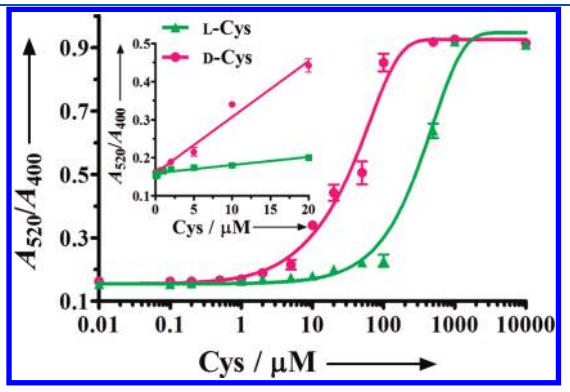

Figure 2. Plots of A_{520}/A_{400} ratio of UTP-capped AgNPs upon the addition of L- and D-Cys at different concentrations (0.01, 0.1, 0.2, 0.5, 1, 2, 5, 10, 20, 50, 100, 500, 1000, and 10 000 μM). Inset: magnification of the plots in the range of 0.0−20 μM. The reaction time was 60 min, and then, the A_{520}/A_{400} ratios were collected.

The aggregation of AgNPs is selectively induced by D-Cys, which allowed the precipitation of D-Cys with AgNPs (Figure 3B) and left a net excess of the other enantiomer in the solution, thus resulting in enantioseparation. Similar to Figure 3C, it was found that no significant UV−vis spectral shift (A_{520}/A_{400}) was detectable in the resultant supernatant (Figure 3D).

Since all of the nucleosides have similar functional groups (amines, carbonyls, etc.) that could act as ligands for the metallic nanoparticle surface as well as phosphate groups along the backbone that could stabilize nanoparticles via electrostatic repulsion, we further exploited the effects of the UTP analogs (ATP, GTP, CTP, and TTP) on the stabilizing AgNPs toward the addition of L- and D-Cys. In our optimized experiment, the best candidate for chiral discrimination of Cys is the UTP-capped AgNPs, which show an appreciable higher A_{520}/A_{400} discrepancy toward L-Cys and D-Cys (Figure S1, Supporting Information).

As shown in Figure S1B (Supporting Information), the ATP-capped AgNPs show negligible discrimination ability toward L-Cys and D-Cys. It was observed that there are gradual decreases in the short-wavelength band (~400 nm) whereas there are gradual increases in the long-wavelength band (~520 nm) with increasing L- or D-Cys concentration (Figure 4A,B). The spectrophotometric changes are accompanied by yellow-to-red color changes (Figure S2, Supporting Information). From Figure 4A,B, it can be seen that the absorption ratio (A_{520}/A_{400}) is sensitive to the concentration of Cys. Therefore, the ATP-capped AgNPs can be used for quantitatively detecting cysteine but not discriminate

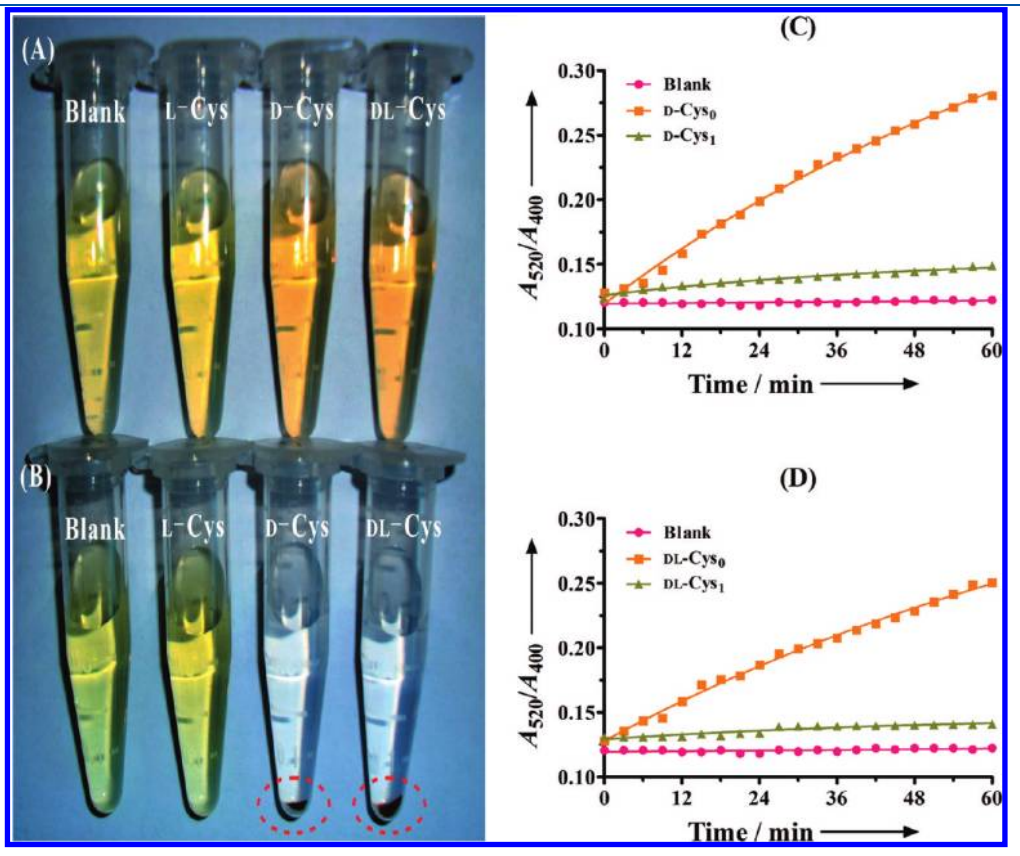

Figure 3. Photo exhibition of UTP-capped AgNPs toward 100 μM L-Cys, D-Cys, and DL-Cys (A) before centrifugation and (B) after centrifugation. Plots of absorption ratios (A_{520}/A_{400}) corresponding to (C) 10 μM D-Cys$_0$ and D-Cys$_1$ (the supernatant of 100 μM D-Cys$_0$ reacted with UTP-capped AgNPs) and (D) 10 μM DL-Cys$_0$ and DL-Cys$_1$(the supernatant of 100 μM DL-Cys$_0$ reacted with UTP-capped AgNPs).

dx.doi.org/10.1021/ac102922f |*Anal. Chem.* 2011, 83, 1504–1509

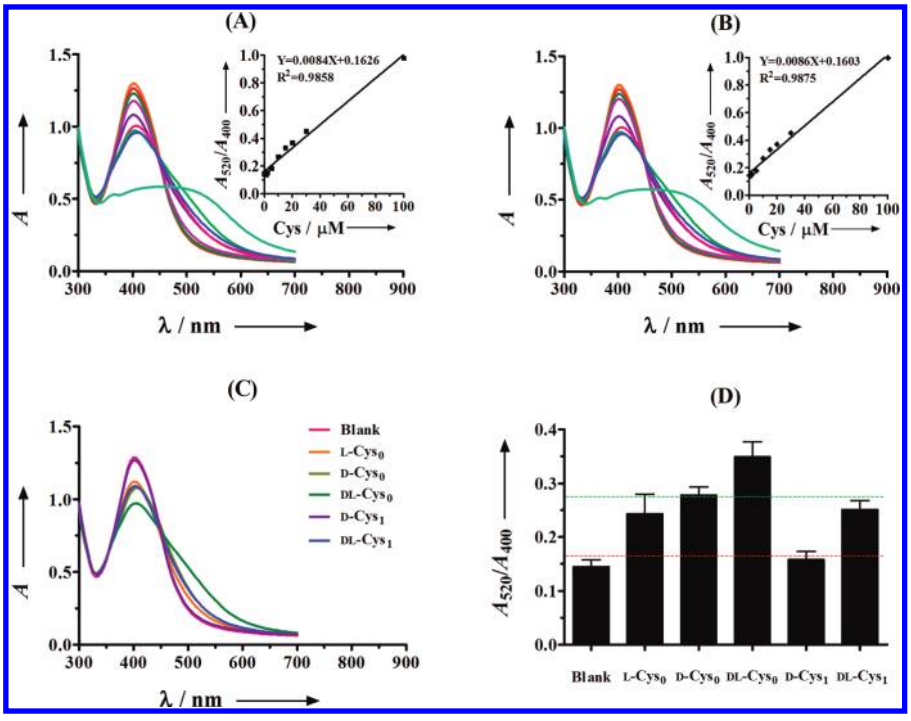

Figure 4. UV−vis absorbance of ATP-capped AgNPs in solution upon addition of (A) L-cysteine and (B) D-cysteine (0, 0.1, 1, 2, 5, 10, 15, 20, 30, and 100 μM), Insets: plots of absorption ratios (A_{520}/A_{400}) corresponding to the varying concentration of cysteine and (C) 10 μM L-Cys_0, D-Cys_0, and D-Cys_1 (the supernatant of 100 μM D-Cys_0 reacted with UTP-capped AgNPs); 10 μM DL-Cys_0, and DL-Cys_1(the supernatant of 100 μM DL-Cys_0 reacted with UTP-capped AgNPs). (D) Bars represent the absorption ratio (A_{520}/A_{400}) of ATP-capped AgNPs in the absence and presence of cysteine (deduced from C).

enantiomers. Moreover, to further test the feasibility of the UTP-capped AgNPs as candidate enantiospecific adsorbents for enantioselective separation and enantiomeric purification of the Cys, the resultant supernatant in D-Cys and DL-Cys tubes was interacted with ATP-capped AgNPs. The results in Figure 4C,D confirmed the same conclusion suggested in the above Figure 3.

CONCLUSIONS

The rational design and construction of optical active ligand-capped nanoparticles for enantioseparation and chiral detection is of intense current interest. In this study, we have developed a novel nanoparticle-based biosensing platform using UTP-capped AgNPs as probe element and demonstrated its feasibility in the application of colorimetric recognition of enantiomers based on absorption chemistry. This novel AgNP-based probe design offers many advantages, including simplicity of preparation and manipulation compared with other methods that employ specific strategies. More importantly, our present sensor can achieve the goal of translating an enantioselective molecular recognition event into an appreciable color change via the aggregation of nanoparticles. This is the first application of a nucleotide-capped AgNP-based biosensing platform for chiral recognition and opens new opportunities for design of more novel enantiosensing strategies and enantiospecific adsorbents and expansion of its application in different fields.

ASSOCIATED CONTENT

Supporting Information. Additional information as noted in text. This material is available free of charge via the Internet at http://pubs.acs.org.

AUTHOR INFORMATION

Corresponding Author

*Fax: (+)00862164252094. E-mail: bcye@ecust.edu.cn.

ACKNOWLEDGMENT

This work was financially supported by NSF21075040, the Shanghai 09JC1404100, NCET-07-0287, SKLBE Fund 2060204, and the Fundamental Research Funds for the Central Universities.

REFERENCES

(1) (a) Mehta, A. C. *J. Clin. Pharm. Ther.* **1990**, *15*, 313. (b) Jiang, Z.; Crassous, J.; Schurig, V. *Chirality* **2005**, *17*, 488. (c) Mohanty, A.; Dey, J. *J. Chromatogr., A* **2006**, *1128*, 259.

(2) James, T. D.; Sandanayake, K. R. A. S.; Shinkai, S. *Nature* **1995**, *374*, 345.

(3) Kubo, Y.; Maeda, S.; Tokita, S.; Kubo, M. *Nature* **1996**, *382*, 522.

(4) (a) Elghanian, R.; Storhoff, J. J.; Mucic, R. C.; Letsinger, R. L.; Mirkin, C. A. *Science* **1997**, *277*, 1078. (b) Thompson, D. G.; Enright, A.; Faulds, K.; Smith, W. E.; Graham, D. *Anal. Chem.* **2008**, *80*, 2805.

(5) (a) Zhao, W.; Chiuman, W.; Lam, J. C.; McManus, S. A.; Chen, W.; Cui, Y.; Pelton, R.; Brook, M. A.; Li, Y. *J. Am. Chem. Soc.* **2008**, *130*, 3610. (b) Han, M. S.; Lytton-Jean, A. K.; Oh, B. K.; Heo, J.; Mirkin, C. A. *Angew. Chem., Int. Ed.* **2006**, *45*, 1807. (c) Liu, J.; Lu, Y. *Angew. Chem., Int. Ed.* **2005**, *45*, 90. (d) Wang, J.; Wang, L.; Liu, X.; Liang, Z.; Song, S.; Li, W.; Li, G.; Fan, C. *Adv. Mater.* **2007**, *19*, 3943.

(6) Tessier, P. M.; Jinkoji, J.; Cheng, Y. C.; Prentice, J. L.; Lenhoff, A. M. *J. Am. Chem. Soc.* **2008**, *130*, 3106.

(7) Scampicchio, M.; Arecchi, A.; Mannino, S. *Nanotechnology* **2009**, *20*, 135501.

(8) (a) Liu, J.; Lu, Y. *J. Am. Chem. Soc.* **2003**, *125*, 6642. (b) Chen, Y. Y.; Chang, H. T.; Shiang, Y. C.; Hung, Y. L.; Chiang, C. K.; Huang, C. C. *Anal. Chem.* **2009**, *81*, 9433.

(9) Gautier, C.; Bürgi, T. *Chem. Phys. Chem.* **2009**, *10*, 483.

(10) (a) Wang, Y.; Yin, X.; Shi, M.; Li, W.; Zhang, L.; Kong, J. *Talanta* **2006**, *69*, 1240. (b) Noguez, C.; Garzon, I. L. *Chem. Soc. Rev.* **2009**, *38*, 757. (c) Shukla, N.; Bartel, M. A.; Gellman, A. J. *J. Am. Chem. Soc.* **2010**, *132*, 8575.

(11) Lee, J. S.; Lytton-Jean, A. K.; Hurst, S. J.; Mirkin, C. A. *Nano Lett.* **2007**, *7*, 2112.

(12) (a) Zeng, J.; Zheng, Y.; Rycenga, M.; Tao, J.; Li, Z. Y.; Zhang, Q.; Zhu, Y.; Xia, Y. *J. Am. Chem. Soc.* **2010**, *132*, 8552. (b) Chen, M.; Feng, Y. G.; Wang, X.; Li, T. C.; Zhang, J. Y.; Qian, D. J. *Langmuir* **2007**, *23*, 5296.

(13) Blackburn, G. M.; Gait, M. J. *Nucleic Acids in Chemistry and Biology*; Oxford University Press: Oxford, UK, 1990.

(14) Zhao, W.; Gonzaga, G.; Li, Y.; Brook, M. A. *Adv. Mater.* **2007**, *19*, 1766.

(15) (a) Ivanov, A. R.; Nazimov, I. V.; Baratova, L. *J. Chromatogr., A* **2000**, *895*, 157. (b) Janaky, R.; Varga, V.; Hermann, A.; Saransaari, P.; Oja, S. S. *Neurochem. Res.* **2000**, *25*, 1397. (c) Hartleb, J.; Arndt, R. *J. Chromatogr., B: Biomed. Sci. Appl.* **2001**, *764*, 409. (d) Soutourina, J.; Blanquct, S.; Plateau, P. *J. Biol. Chem.* **2001**, *276*, 40864. (e) Lim, I. I.; Mott, D.; Engelhard, M. H.; Pan, Y.; Kamodia, S.; Luo, J.; Njoki, P. N.; Zhou, S.; Wang, L.; Zhong, C. J. *Anal. Chem.* **2009**, *81*, 689.